RSC Advances

REVIEW

Cite this: *RSC Adv.*, 2022, **12**, 810

Bright red emission with high color purity from Eu(III) complexes with π-conjugated polycyclic aromatic ligands and their sensing applications†

Yuichi Kitagawa, *[ac] Makoto Tsurui[b] and Yasuchika Hasegawa *[ac]

Received 10th November 2021
Accepted 18th December 2021

DOI: 10.1039/d1ra08233g

rsc.li/rsc-advances

Eu(III) complexes emit red light with a high color purity and have consequently attracted attention for development toward display and physical sensing applications. The characteristic pure color emission originates from the intra-4f–4f transition, and the brightness strongly depends on the electronic and steric structures of organic ligands. A large π-conjugated ligand design with a large absorption coefficient has been actively studied for achieving bright emission. The π-conjugated Eu(III) luminophores also provide oxygen and temperature sensing properties by controlling their excited state dynamics based on π-electron systems. A comprehensive understanding of the design strategy of large π-conjugated ligands is crucial for the further development of luminescent Eu(III) complexes. In this review, we summarize the research progress on π-conjugated Eu(III) luminophores exhibiting bright emission and their physical sensing applications.

1 Introduction

Highly bright monochromatic luminescent compounds have become increasingly important for the development of display and sensing materials. A considerable number of studies have been conducted on the development of various luminescent compounds such as luminescent organic dyes,[1–4] metal complexes,[5–7] and inorganic compounds (nanoparticles and ceramics).[8–15] Recently, Hatakeyama *et al.* successfully prepared a blue luminescent boron-based organic dye with high color purity (full-width at half-maximum (FWHM) of 28 nm) for the fabrication of efficient organic light emitting diodes (LEDs).[16] Jang *et al.* prepared InP/ZnSe/ZnS quantum dots exhibiting strong red luminescence with high color purity (FWHM of 35 nm).[17] Xia *et al.* synthesized the $RbNa_3(Li_3SiO_4)_4:Eu^{2+}$ phosphor that exhibited a narrow red emission band (FWHM of 22.4 nm).[18] Besides these luminescent systems, Eu(III) complexes have emerged as a promising candidate for achieving characteristic pure red luminescence (Fig. 1a, FWHM ≈ 10 nm).[19–23]

Eu(III) complexes are organic–inorganic hybrid compounds in which organic ligands are attached to the Eu(III) center. The Eu(III) ion has an incompletely filled 4f orbital, which is shielded by the outer shells such as the filled $5s^2$ and $5p^6$ orbitals. In a configurational coordinate diagram, these levels appear as parallel parabolas (a small offset case: Fig. 1b) because the 4f electrons are well shielded from their surroundings.[24] Therefore, sharp emission lines (FWHM ≈ 10 nm) corresponding to the $^5D_0 \rightarrow {}^7F_J$ ($J = 0$, 1, 2, 3, 4, 5, and 6) transitions are observed. Among these, the $^5D_0 \rightarrow {}^7F_2$ transition is dramatically affected upon changing the ligand field, and pure red emission can be obtained using appropriate ligands. Eu(III) ions exhibit extremely weak absorption (molar absorption coefficient (ε) < 5 M^{-1} cm^{-1}).[25] This limitation can be overcome by using organic compounds with high light-harvesting ability ($\varepsilon = 10^3$ to 10^5 M^{-1} cm^{-1}) as ligands in the Eu(III) complexes. Eu(III) complexes with such ligands can exhibit strong luminescence through energy transfer from the organic ligands to the metal center.

The brightness of Eu(III) complexes is a key factor in the development of Eu(III)-based luminescent materials. Brightness is defined as the product of the light absorption coefficient and emission quantum yield. The brightness (I_B) is expressed as follows:[26]

$$I_B = \varepsilon \times \Phi_{tot} = \varepsilon \times \eta_{sens} \times \Phi_{ff} = \varepsilon \times \eta_{sens} \times \frac{k_r}{k_r + k_{nr}},$$

Here, ε and Φ_{tot} are the absorption coefficient of the organic ligand and the quantum yield of the Eu(III) emission excited by organic ligand, respectively. η_{sens}, Φ_{ff}, k_r, and k_{nr} are the efficiency of sensitization, Eu(III)-centered luminescence quantum yield, radiative rate constant, and non-radiative rate constant,

[a]*Faculty of Engineering, Hokkaido University, N13W8, Kita-ku, Sapporo, Hokkaido 060-8628, Japan. E-mail: y-kitagawa@eng.hokudai.ac.jp; hasegaway@eng.hokudai.ac.jp*

[b]*Graduate School of Chemical Sciences and Engineering, Hokkaido University, N13W8, Kita-ku, Sapporo, Hokkaido 060-8628, Japan*

[c]*Institute for Chemical Reaction Design and Discovery (WPI-ICReDD), Hokkaido University, N21 W10, Kita-ku, Sapporo, Hokkaido 001-0021, Japan*

† Electronic supplementary information (ESI) available: Chemical structures and photophysical parameters of Eu(III) complexes (photophysical parameters of several Eu(III) complexes are not available). See DOI: 10.1039/d1ra08233g

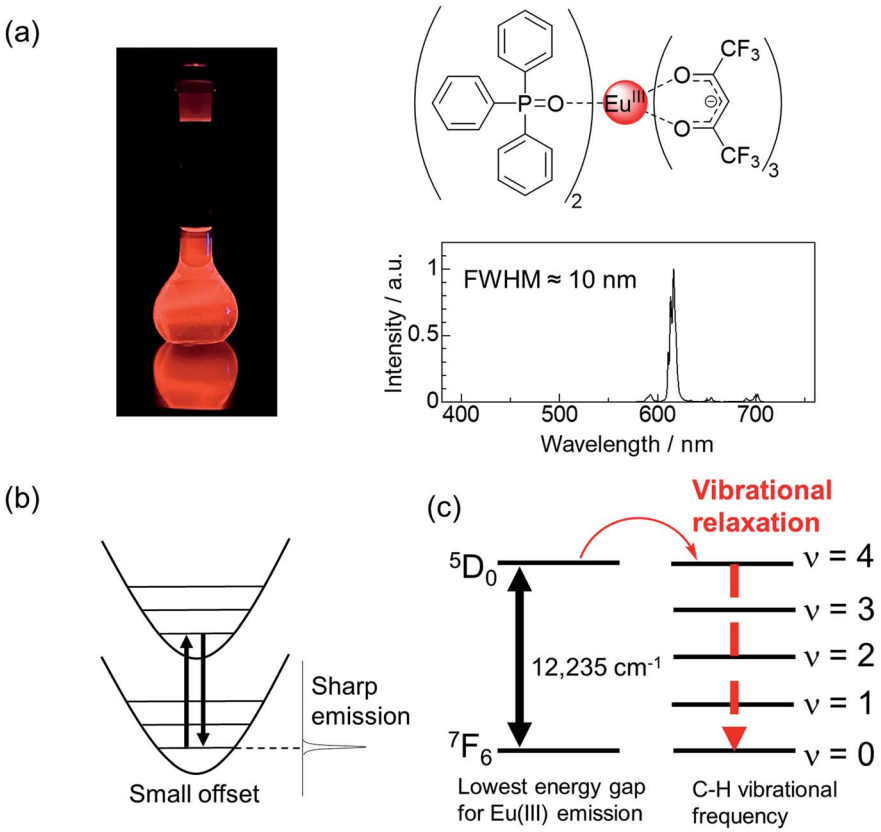

Fig. 1 (a) Emission photograph, chemical structure of a highly luminescent Eu(III) complex, and its emission spectrum. (b) Emission due to 4f–4f transition in Eu(III) ions. (c) Matching of the vibrational overtone of the C–H bonds in the Eu(III) complex.

respectively. To achieve high brightness, molecular designing must focus on achieving high ε, η_{sens}, and Φ_{ff}.

Eu(III) complexes containing an anionic β-diketonate ligand (*e.g.*, thenoyltrifluoroacetonate (tta) or hexafluoroacetylacetonate (hfa) ligand) with large polarizability have a large k_r value,[27,28] and exhibit efficient energy transfer to the Eu(III) center.[29,30] Asymmetric coordination geometries originating due to the presence of anionic ligands and neutral ligands are also a key factor in increasing k_r, as they promote the mixing of the 4f–5d excited states with the 4f–4f excited states.[31,32] The non-radiative deactivation of the Eu(III) emissive states is promoted by proximate energy-matched OH, NH, and CH oscillators (*e.g.*, water, methanol, and amine; high vibrational frequency, >3000 cm^{-1}, Fig. 1c).[33,34] Thus, neutral ligands (*e.g.*, phosphine oxide) with low vibrational frequencies provide small k_{nr} by suppressing vibrational quenching. From the viewpoint of k_r and k_{nr}, it is evident that Eu(III) complexes containing β-diketonate ligands and low vibrational neutral ligands (*e.g.*, Fig. 1a) are effective for achieving high emission quantum yields.[35]

Improving the light harvesting ability is the key to enhance the brightness of Eu(III) luminophores. Several large π-conjugated systems have extremely high absorption coefficients (ε_{max} > 10^5 M^{-1} cm^{-1}).[36] A comprehensive understanding of the design strategies for large π-conjugated ligands is crucial for the development of efficient luminescent Eu(III) complexes. In this review, we have summarized the research progress and physical sensing properties of π-conjugated Eu(III) complexes that exhibit bright emission.

2 Historical interpretation of the efficient energy transfer from ligand-to-Eu(III)

First, we discuss the historical interpretation of the efficient energy transfer from the ligand to Eu(III) ions. The UV-light-sensitized luminescence of Eu(III) complexes with organic ligands was observed by Weissman in 1942.[37] Based on the finding, organic ligands were designed for the preparation of strong luminescent Eu(III) complexes. The organic ligands undergo intersystem crossing (ISC) from the lowest singlet excited state (S_1) to the lowest triplet excited state (T_1) after excitation, thereby transferring their electronic energy to the Eu(III) ion (Fig. 2a). Eu(III) ions have several states ($^5D_0$: 17 250 cm^{-1}, $^5D_1$: 19 000 cm^{-1}, and $^5D_2$: 21 500 cm^{-1}) that can accept the energy. In 1970, Sato and coworkers demonstrated the importance of the T_1 state for energy transfer to the $^5D_1$ level in Eu(III) complexes with β-diketonate ligands.[38] They showed that the emission quantum yield due to ligand excitation reached a maximum when the T_1 level was ~1200 cm^{-1} above the $^5D_1$ level. Latva and coworkers performed a further detailed

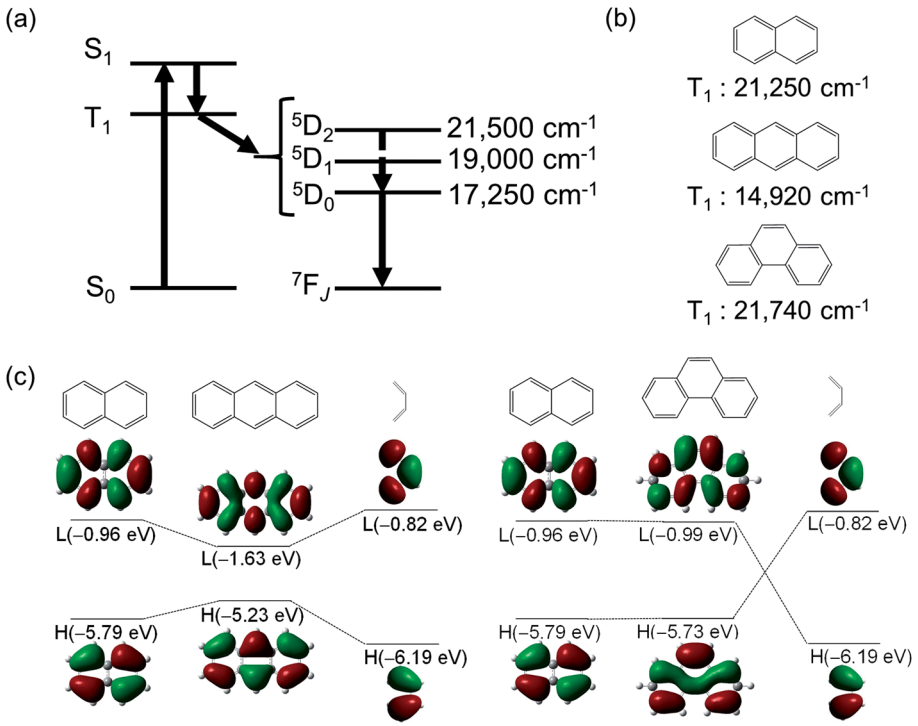

Fig. 2 (a) Energy level diagrams of luminescent Eu(III) complex. (b) T_1 energy levels of naphthalene, anthracene, and phenanthrene. (c) Fragment molecular orbitals for anthracene and phenanthrene. Redrawn from ref. 44.

investigation of the energy transfer using amino-carboxylate-type ligands.[39] They showed a clear relationship between the emission quantum yield (due to ligand excitation) and the T_1 energy level. The results showed that the $^5D_2$ level of the Eu(III) ion could also accept energy. These studies[38,39] suggested that the T_1 state should be higher in energy than the $^5D_1$ state (19 000 cm^{-1}) for effective energy transfer.

The T_1 states of aromatic benzene, naphthalene, and anthracene lie at 29 470 cm^{-1}, 21 250 cm^{-1}, and 14 920 cm^{-1}, respectively (Fig. 2b).[36] The T_1 level of anthracene (14π-electron system) is lower than the emitting levels of Eu(III). In contrast, the T_1 level of ligands such as phenanthrene, which has the same π-conjugation length (14π-electron), is higher (Fig. 2b, >19 000 cm^{-1}) and facilitates photosensitized energy transfer to Eu(III) ions.[40,41] This suggests that the extension of π-conjugation to tailor the T_1 levels of ligands can broaden the scope of ligand design. Using the fragment molecular orbital method and DFT calculations (B3LYP/6-31G(D)[42,43]),[44] we have previously shown a simple method for manipulating the T_1 energy level.

The energy of the T_1 level ($\Delta E(T_1)$) is expressed as follows:

$$\Delta E(T_1) = E(T_1) - E(S_0) = \varepsilon_f - \varepsilon_i - J_{if} \quad (1)$$

Here, ε is the orbital energy, and J is the Coulomb integral representing the electrostatic repulsion due to orbital charge distributions. Subscripts i and f denote the occupied and unoccupied orbitals related to the T_1 state, respectively. As the π-conjugated system is extended, the J_{if} value tends to decrease due to increased delocalization of the electron density. Establishing a molecular design for ineffective orbital energy change related to the T_1 states allows the T_1 level to be maintained.

As a standard for π-conjugated molecules, we used naphthalene, whose excited state energy ($\Delta E(T_1)$ = 21 250 cm^{-1}) is higher than the emission levels of Eu(III) ions. Extending the π-conjugation by coupling naphthalene and butadiene affords anthracene or phenanthrene. The HOMOs of naphthalene and butadiene (−5.79 and −6.19 eV, respectively) and their LUMOs (−0.96 and −0.82 eV, respectively) are electronically coupled in-phase, resulting in a more destabilized HOMO (−5.23 eV) and more stabilized LUMO (−1.63 eV) for anthracene (Fig. 2c, left). This smaller HOMO–LUMO energy gap yields a low T_1 level for anthracene (14 920 cm^{-1}). However, for phenanthrene (Fig. 2c, right), the HOMOs and LUMOs of naphthalene and butadiene are electronically coupled in such a manner that the HOMO (−5.73 eV) and LUMO (−0.99 eV) energies are almost unchanged relative to those of naphthalene. Consequently, the T_1 level of phenanthrene was nearly unchanged ($\Delta E(T_1)$ = 21 740 cm^{-1}).[45] Thus, controlling the electronic structure can maintain the T_1 level at an appropriate position in extended π-conjugation systems. Conjugated systems with more than 18 π electron, such as [4]-helicene ($\Delta E(T_1)$ = 19 870 cm^{-1}),[46] triphenylene ($\Delta E(T_1)$ = 23 580 cm^{-1}),[47] chrysene ($\Delta E(T_1)$ = 20 000 cm^{-1}),[47] [5]-helicene ($\Delta E(T_1)$ = 19 750 cm^{-1}),[46] picene ($\Delta E(T_1)$ = 20 010 cm^{-1}),[48] [6]-helicene ($\Delta E(T_1)$ = 18 990 cm^{-1}),[46] coronene ($\Delta E(T_1)$ = 19 400 cm^{-1}),[47] and phenacene ($\Delta E(T_1)$ = 19 380 cm^{-1}),[48] have relatively high T_1 energies (Fig. 3). Among these, luminescent Eu(III) complexes with triphenylene,[49–53]

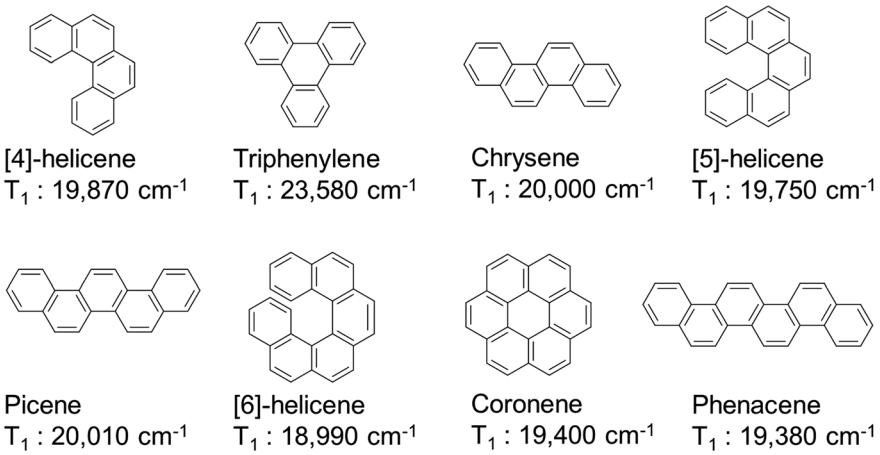

Fig. 3 T_1 energy levels of polycyclic aromatic hydrocarbon.

chrysene,[54–56] [5]-helicene,[44] picene,[57] and coronene[58,59] frameworks have already been reported (chemical structures and their photophysical properties are shown in Fig. S1 and S2 in the ESI†). Several hetero-conjugated systems,[60–82] such as 1,4,8,9-tetraazatriphenylene ($\Delta E(T_1) = 23\ 500\ cm^{-1}$), are well known to possess high T_1 energy for photosensitized Eu(III) emission (chemical structures and their photophysical properties are shown in Fig. S3–S9 in the ESI†). These appropriate T_1 levels are expected to facilitate photoinduced energy transfer to Eu(III) ions. The S_1 energy of a molecule is expressed as follows:

$$\Delta E(S_1) = E(S_1) - E(S_0) = \varepsilon_f - \varepsilon_i - J_{if} + 2K_{if} \quad (2)$$

Here, K is the exchange integral between the orbital pairs. The extended π-conjugated ligands possess a relatively small energy gap between the S_1 and T_1 states, as evident from the small exchange integral,[83] leading to low-energy light absorption.[84]

3 Photophysics of Eu(III) complexes with large π-conjugated systems and their applications

Eu(III) complexes with β-diketonate ligands have a high radiative rate constant and high color purity emission due to the strong $^5D_0 \rightarrow {}^7F_2$ electronic dipole transition. In this section, we mainly review the photophysics of extended π-conjugated Eu(III) complexes with β-diketonate ligands and their applications.

3.1 Basic photophysical properties of Eu(III) complexes with large π-conjugated system

3.1.1 UV-light sensitized Eu(III) emission. There are several reports on Eu(III) complexes with an extended π-conjugated system containing benzene, naphthalene, and phenanthrene frameworks; as discussed before, such system facilitate effective energy transfer to Eu(III) ions.[38,85–87] Recently, the photophysical properties of Eu(III) complexes bearing hexafluoroacetylacetonate ($\Delta E(T_1) = 22\ 200\ cm^{-1}$), 4,4,4-trifluoro-1-phenyl-1,3-butanedione ($\Delta E(T_1) = 21\ 400\ cm^{-1}$), or 3-(2-naphthoyl)-1,1,1-trifluoroacetonate ($\Delta E(T_1) = 19\ 600\ cm^{-1}$) ligands and neutral ligand with a low vibrational frequency (bis[2-(diphenylphosphino)phenyl]ether oxide),[88] were investigated in detail (Fig. 4a–c, Eu-hfa, Eu-btfa, and Eu-ntfa). The thermal stability (thermal decomposition point: T_d) of the Eu(III) complexes bearing the extended π-conjugated ligands (T_d = 320 °C and 318 °C for Eu-btfa and Eu-ntfa, respectively) was much higher than that of Eu-hfa (T_d = 228 °C). The longest absorption edge was observed for Eu-ntfa (394 nm), followed by Eu-btfa (380 nm) and Eu-hfa (361 nm); this order was consistent with the length of the π-conjugation. In contrast, the emission quantum yields of π-extended Eu(III) complexes Eu-btfa (Φ_{tot} = 38%) and Eu-ntfa (Φ_{tot} = 45%) were lower than that of Eu-hfa (Φ_{tot} = 57%). The lower emission quantum yield in a large π-conjugated system can be attributed to the increased non-radiative rate constants (k_{nr} = 280, 340, and 590 s^{-1} for Eu-hfa, Eu-btfa, and Eu-ntfa, respectively). k_{nr} is affected by secondary vibrational quenching due to the high C–H vibrational frequency of aromatic units in electronically delocalized β-diketonate ligands (Fig. 4d). The effect on k_{nr} owing to vibrational quenching originating from the β-diketonate ligand was also demonstrated by a deuterium replacement experiment in hfa ligands.[35] Thus, a π-extended β-diketonate ligand containing aromatic moieties is not a reasonable ligand for Eu(III) complexes with high 4f–4f emission quantum yields.

Based on the photophysical properties of Eu(III) complexes with the β-diketonate ligand, we focused on the electronic separation between the energy-donating aromatic orbital and the energy-accepting Eu(III) orbital *via* a phosphine spacer with a low vibrational frequency (Fig. 4e).[52] This electronic separation is expected to suppress the vibrational relaxation of the Eu(III) ion and lower the rate of energy transfer. To construct an efficient energy transfer system based on the weak electronic interaction between the energy donor (aromatic ligand) and energy acceptor (Eu(III)), a triphenylene unit with high triplet state (T_1) energy and long lifetime was employed. Thus, we designed an Eu(III) complex with low vibrational frequency hfa ligand and phosphine oxide ligand containing triphenylene frameworks. The crystal structure is shown in Fig. 4f. The intra-

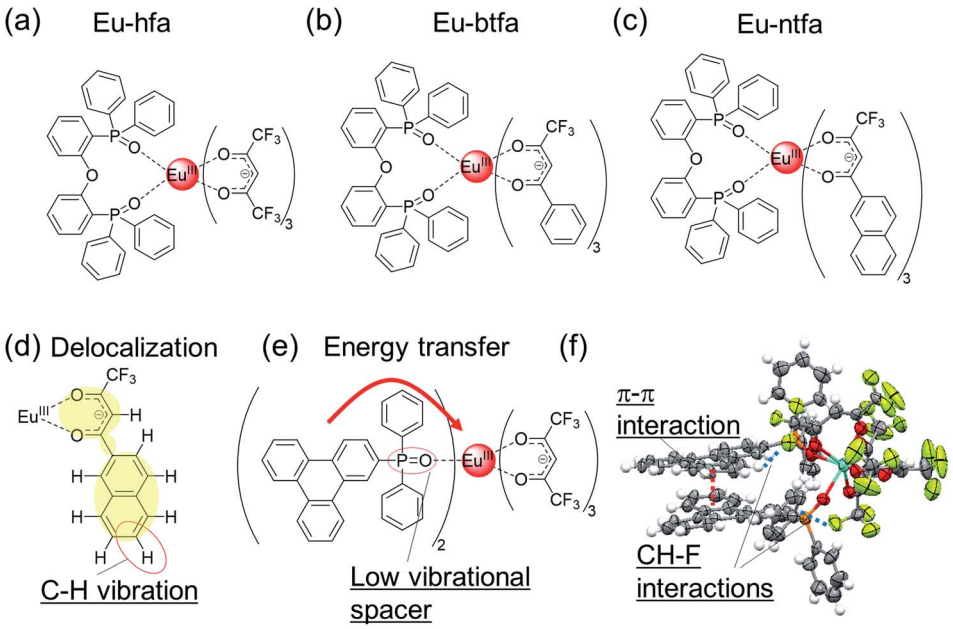

Fig. 4 Chemical structures of (a) Eu-hfa, (b) Eu-btfa, and (c) Eu-ntfa. (d) Delocalization in Eu-ntfa. (e) Eu(III) complex with triphenylene frameworks. (f) X-ray crystal structure (ORTEP drawings) of Eu(III) complex with triphenylene frameworks. Redrawn from ref. 52.

and intermolecular π–π (3.3 Å, triphenylene ligand/triphenylene ligand) and CH–F (2.6–2.9 Å, triphenylene ligand/hfa ligand) interactions result in the formation of a rigid structure, endowing high thermal stability (T_d = 310 °C) by suppressing the dissociation of the hfa ligand. The UV light absorption ability of the triphenylene ligand (ε > 100 000 cm^{-1} M^{-1}) is much higher than that of the hfa ligand. The emission quantum yield owing to ligand excitation was estimated to be 63% (in CH_2Cl_2); thus, the Eu(III) complexes have remarkable thermal stability and exhibit high brightness. The detailed energy transfer mechanism in the triphenylene-based highly luminescent Eu(III) complex was revealed by time-resolved spectroscopy,[89] which provides useful information on photosensitized energy transfer mechanism in luminescent Eu(III) complexes.

3.1.2 Blue-light sensitized Eu(III) emission. Blue-light sensitized Eu(III) emission is advantageous as it can suppress UV-light-induced phototoxicity in living beings.[90] In particular, Eu(III) emission has attracted attention with regard to the development of LED chip-based displays.[91–93] However, achieving blue light-sensitized Eu(III) luminescence in low-concentration states of matter (*i.e.*, not solid states) is still a challenging task in lanthanide photochemistry. The photosensitized emission *via* the triplet state results in energy loss during intersystem crossing ($\Delta E_{S_1-T_1}$). In addition, a high T_1 level is essential for suppressing the photon loss caused by the back energy transfer from the energy-accepting state to T_1 ($\Delta E_{T_1-{}^5D_0}$). Thus, the energy transfer mechanism involves two energy loss processes ($\Delta E_{S_1-T_1}$ and $\Delta E_{T_1-{}^5D_0}$), thus making it difficult for application to blue light excitation (Fig. 5a).

Gong *et al.* successfully demonstrated blue light-sensitized emission from Eu(III) complexes bearing extended π-conjugated β-diketonate ligand containing carbazole frameworks (Fig. 5b, left).[94] A characteristic pure red-emitting diode was fabricated by coating the complex phosphor onto a ~460 nm-emitting InGaN chip. The emission quantum yield owing to ligand excitation was estimated to be 16%. The relatively low yield can be attributed to the low T_1 level (18 800 cm^{-1}; below the $^5D_1$ level). Koizuka *et al.* successfully prepared Eu(III) complexes with hfa and *N*,*N*′-bis(salicylidene)-1,4-butanediamine ligands, which could be excited by a blue LED chip (Fig. 5b, right, $\varepsilon_{450\ nm}$ = 190 M^{-1} cm^{-1}, Φ_{tot} = 47%).[95] The blue light absorption was dependent on the effective electronic interactions between the hfa ligands and *N*,*N*′-bis(salicylidene)-1,4-butanediamine.

Chen *et al.* prepared a blue light-sensitized Eu(III) complex using an Ir(III) complex photosensitizer (Fig. 5c, $\varepsilon_{450\ nm}$ = 600 M^{-1} cm^{-1}, Φ_{tot} = 18%).[96] The excitation window extended up to 530 nm, which can be related to the effective S–T transition, without any energy loss due to ISC ($\Delta E_{S_1-T_1}$). The S–T transition is the key to photosensitization *via* the triplet states for enabling low-energy light excitation for photochemical processes.[97–99] The T_1 energy level (21 200 cm^{-1}) of the Ir(III)-based photosensitizer is appropriate for efficient energy transfer. Despite this, the emission quantum yield owing to ligand excitation was relatively low (Φ_{tot} = 18%). This can be attributed to the rapid deactivation of T_1 due to the heavy-atom effect (T_1 lifetime of photosensitizer, τ < 0.15 ms), leading to ineffective energy transfer from T_1 to $^5D_1$.

Recently, we reported the highest brightness in blue light sensitized Eu(III) complexes prepared using a stacked nanocarbon photosensitizer (Fig. 5d, $\varepsilon_{450\ nm}$ = 1700 cm^{-1} M^{-1}, Φ_{tot} = 36%).[59] The two nanocarbon ligands are located between Eu(III) centers and form intramolecular π–π interactions (3.5 Å). The

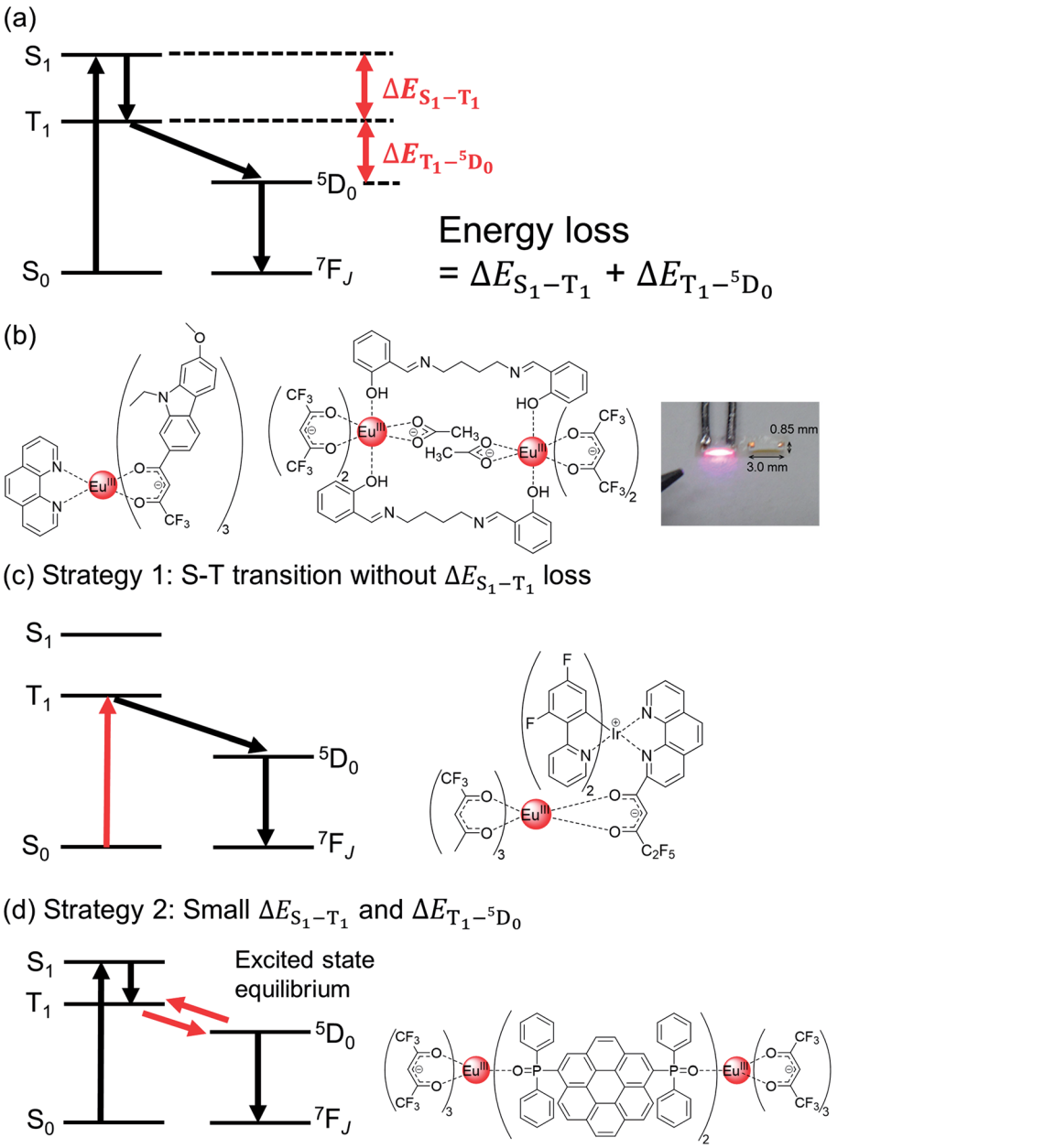

Fig. 5 (a) Energy diagram showing energy loss during photosensitized Eu(III) emission; (b) Eu(III) complex with carbazole framework (left), Eu(III) complex with *N*,*N*′-bis(salicylidene)-1,4-butanediamine and its luminescence image of LED package (right). Redrawn from ref. 95 Copyright (2018) American Chemical Society. (c) Schematic energy diagram for S–T transition (left) and Eu(III) complex with Ir(III) complex photosensitizer (right). (d) Schematic energy diagram for excited state equilibrium (left) and Eu(III) complex with stacked nanocarbon photosensitizer (right).

stacked nanocarbon ligands are surrounded by hfa ligands, forming effective intramolecular CH–F interactions (3.0 Å). The photosensitized T_1 level (18 800 cm^{-1}) was lower than that of the $^5D_1$ level, and the back energy transfer occurred from $^5D_0$ to T_1. Notably, the nanocarbon photosensitizers in rigid environments have a longer T_1 lifetime (40 ms) compared to that of the Eu(III) ion (~1 ms). The long T_1 lifetime is expected to facilitate the efficient use of photons even in the case of low T_1 levels, with an excited state equilibrium between $^5D_0$ and T_1. The excited state equilibrium was confirmed from the emission lifetime measurements based on the oxygen concentrations[100,101] (Ar: 0.7 ms, Air: 0.5 ms). The large π-conjugated nanocarbon also induces a small $\Delta E_{S_1-T_1}$ (=3700 cm^{-1}, $\Delta E(S_1)$ = 22 600 cm^{-1}). Thus, the stacked nanocarbon with long-lived photons and small $\Delta E_{S_1-T_1}$ and $\Delta E_{T_1-^5D_0}$ energy gaps aids in low-energy light absorption and efficient energy transfer.[102]

3.2 Physical sensing applications of Eu(III) complexes with large π-conjugated system

3.2.1 Temperature sensing. Thermosensitive paints are next-generation analytical tools for measuring the surface

temperatures of various substances. Luminescent molecular paints, in particular, have attracted considerable attention because of their high detection sensitivity and short response time.[103–106] Eu(III) complexes are promising materials for preparing luminescent paints because of their narrow red emission bands arising from the 4f–4f transitions (FWHM ≈ 10 nm) and long emission lifetimes (>1 μs), which allow precise temperature imaging.[19–22] Both high optical brightness and excellent temperature sensitivity are essential for constructing an effective molecular thermometer. Recently, Belluci *et al.* successfully prepared dinuclear Eu(III) complexes with β-diketonate ligands (tta [thenoyl trifluoroacetonate], btfa [benzoyltrifluoroacetonate], dbm [dibenzoylmethane], and hfa [hexafluoroacetylacetonate]) and *N*-oxide ligands (pyradine N-oxide) (Fig. 6a).[107] These dinuclear Eu(III) complexes exhibited efficient photosensitized emission properties and effective temperature-dependent emission intensity changes, originating from both ligand-to-metal charge transfer (LMCT) and localized ligand T_1 quenching sites.

On the other hand, emission lifetime-based thermometers and ratiometric luminescence thermometers are not sensitive to variations in the luminophore concentration, its surrounding environment, or the sample viscosity. Wolfbeis *et al.* prepared luminescent Eu(III) nanoparticles with extended π-conjugated β-diketonate ligands for sensing and imaging temperature in the physiological range (Fig. 6b).[108] We also demonstrated emission lifetime-based thermometers of the Eu(III) complexes with hfa and chrysene frameworks, which exhibited an extremely high molar absorption coefficient (490 000 cm^{-1} M^{-1}) in the UV region, a high intrinsic emission quantum yield (73%), and temperature-dependent energy transfer between ligands and Eu(III) ions (Fig. 6c).[55] The characteristic energy transfer was explained by the LMCT based on π–f orbital interactions. The high thermostability (T_d = 281 °C) was attributed to the multiple CH–F interactions, as evident from the crystal structure. This high thermostability is advantageous for developing molecular thermometers. The long range π–4f interactions in the chrysene frameworks were also investigated using an Eu(III) coordination polymer (Fig. 6d).[56] The single polymer chains show the characteristic zig-zag orientation, inducing multiple CH–F interactions, and exhibit higher thermal stability (T_d = 358 °C) than the mononuclear Eu(III) complex. The relative thermal sensitivity (S_m) of the Eu(III) coordination polymer with chrysene linkers was higher (S_m = 2.70% K^{-1} at 475 K) than those of mononuclear Eu(III) complexes (S_m = 0.89% K^{-1} at 475 K). The extent of LMCT delocalization was controlled by doping with Gd(III) ion, which resulted in an increased emission quantum yield and thermal sensitivity (S_m = 3.70% K^{-1} at 475 K). Thus, a luminescence-lifetime-based thermometer of Eu(III) complexes with high brightness, high thermostability, and high thermo-sensitivity was successfully demonstrated. The study on Eu(III) LMCT excited states of the ligand (π)- and 4f-orbitals is relatively unestablished; thus, the results also provide an useful information for future Eu(III) photo-physics study.[109]

Eu(III)-based ratiometric luminescence has also been utilized for the construction of effective thermometers. Historically, the most common case is the ratiomteric emission using coordination polymers composed of red-luminescent Eu(III) and green-luminescent Tb(III) centers (Fig. 6e, left).[110,111] The mixed Eu(III)–Tb(III) coordination polymers exhibit strong green, yellow, orange, and red luminescence under UV irradiation (365 nm) at 250, 300, 350, and 400 K, respectively (Fig. 6e, right), which is mainly based on the temperature-dependent back energy transfer from Tb(III) to organic ligand.[111] Both Eu(III) and Tb(III) exhibited long emission lifetimes (sub-millisecond), allowing for characteristic time-gated detection.[112] There are several reports of ratiometric emission originating from Eu(III) phosphorescence and ligand fluorescence.[113–115] Vaidyanathan *et al.* prepared five novel Eu(III) complexes with dibenzoylmethanate and phenantro-imidazole derivatives (Fig. 6f).[114] The asymmetric hetero-conjugated system endowed additional fluorescence properties, and the five Eu(III) complexes could be utilized for thermometry owing to the ratiometric emission originating from Eu(III) phosphorescence and ligand fluorescence. In particular, the Eu(III) complex with a 4-(trifluoromethyl)phenyl substituent behaves as an effective ratiometric temperature sensor in the temperature range of 303–353 K, with a relative sensitivity of 1.97% K^{-1} at 313 K. Achieving high emission quantum yields in Eu(III) complexes with dual luminescence (Eu(III) phosphorescence and ligand fluorescence) is difficult (<20%, in ref. 114). Recently, it has been demonstrated that the emission quantum yield could be improved by changing the β-diketonate ligands (Fig. 6g, $\Phi \approx$ 24%).[115] These phenantro-imidazole based Eu(III) complexes are also shown to have versatile luminescent applications, such as vapour sensors and white LED, using the dual luminescent properties.[113–124]

3.2.2 Oxygen-based sensing. Oxygen sensing techniques are employed in various fields such as clinical analysis and environmental monitoring.[125–127] Molecular triplet states are quenched by triplet oxygen, and singlet oxygen is generated. Thus, the luminophore-based oxygen sensing technique is based on phosphorescence quenching or excited triplet state quenching in a photosensitizer (Fig. 7a, left). In the former case, the metal-to-ligand (or ligand-to-metal) charge transfer phosphorescence in transition metal complexes, such as Ir(III), Ru(II), or Pt(II) complexes, has been reported for effective oxygen sensing.[128–130] In the latter case, the Eu(III) luminescence is based on the energy transfer from the T_1 state of the photosensitizer to the excited state of Eu(III) (Fig. 7a, left). Amao *et al.* presented the first oxygen sensor using a luminescent Eu(III) complex based on oxygen quenching in the T_1 state of the β-diketonate ligand (Fig. 7a, right).[131] In the other cases, the Eu(III) emission using a photosensitizer with a short T_1 lifetime was not sensitive to oxygen (Fig. 7b, left). Using this property, Khalil *et al.* demonstrated the ratiometric emission based on an Eu(III) complex with a large π-conjugated system containing a phenanthrene framework, which was non-sensitive to oxygen, and a Pt(II) porphyrin, which exhibited high oxygen sensitivity (Fig. 7b, right).[132] Because the 4f–4f excited states are not directly affected by oxygen, the 4f–4f emission lifetime remains unchanged. Based on the excited state equilibrium between the T_1 state and $^5D_0$ (emitting) state, we demonstrated that the effective emission lifetime could change in Eu(III) complexes

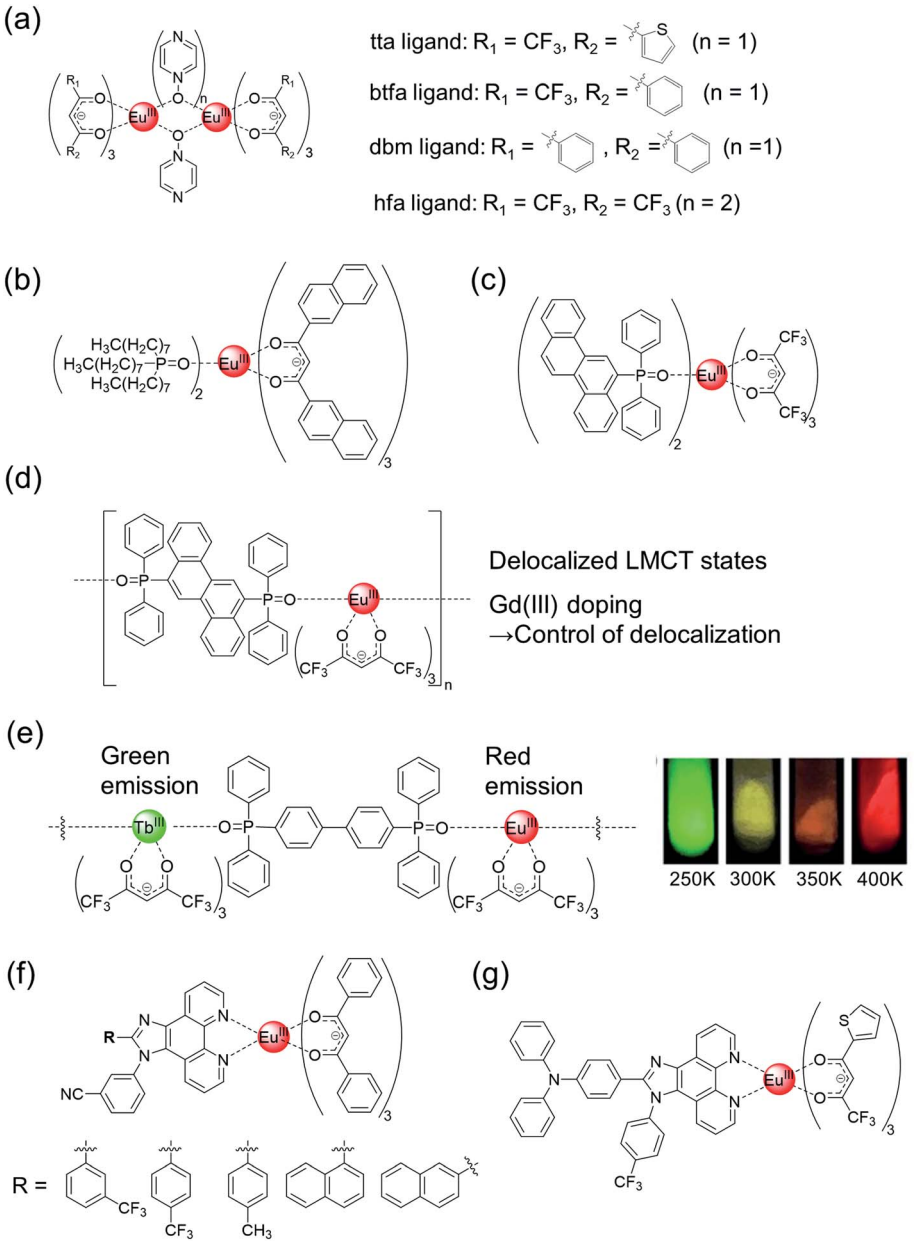

Fig. 6 Chemical structures of Eu(III) complexes with (a) emission-intensity-based thermometer property and (b and c) emission-lifetime-based thermometer property. Chemical structures of Eu(III) coordination polymers with (d) emission-lifetime-based thermometer property and (e, left) ratiometric (Eu(III)/Tb(III))-emission-based thermometer property. (e, right) Emission photograph of Eu(III)/Tb(III) (1/99) coordination polymer under UV (365 nm) irradiation. Redrawn from ref. 111, Copyright (2013) Wiley-VCH Verlag GmbH & Co. KGaA, Weinheim. (f and g) Chemical structures of Eu(III) complexes with ratiometric (Eu(III)/ligand)-emission-based thermometer property.

with a triphenylene framework, depending on the oxygen concentration (Fig. 7c).[53] The small energy gap between excited T_1 and emitting levels ($^5D_0$) is 1650 cm^{-1} for the effective back energy transfer is a key point for the lifetime-based oxygen sensor using the excited state equilibrium.

The singlet oxygen generated by triplet quenching has also received attention because of its vital role in biological and environmental systems. Song *et al.* reported a visible light-excitable Eu(III) complex-based luminescent probe, which contains 2-(*N*,*N*-diethylanilin-4-yl)-4,6-bis(3,5-dimethylpyrazol-1-yl)-1,3,5-triazine as a photosensitized ligand and β-diketonate with anthracene as the reactive part (Fig. 7d).[133] Anthracene reacts with the singlet oxygen generated by energy transfer from triplet anthracene to triplet oxygen. The T_1 level of the anthracene unit is lower than the emitting level of Eu(III). The Eu(III) emission is strongly quenched by the β-diketonate-containing anthracene framework; however, Eu(III) shows strong emission due to the oxidization reaction because of the high T_1 level in oxidized anthracene. This Eu(III) complex can also specifically localize in the mitochondria of live cells. This allows it to be used for tracing the generation of $^1O_2$ in the mitochondria of living cells. The long emission lifetime of

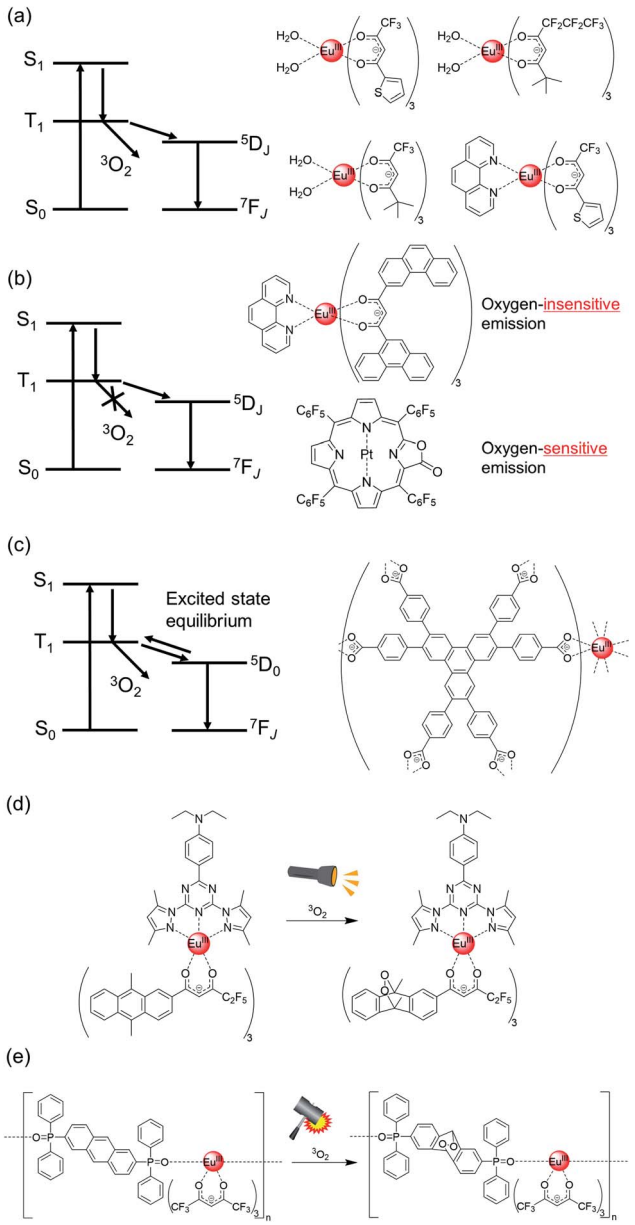

Fig. 7 (a) Schematic energy diagram showing the quenching of T_1 state by $^3O_2$ (left) and chemical structure of Eu(III) complex with oxygen-sensitive emission (right). (b) Schematic energy diagram wherein the T_1 state is not quenched by $^3O_2$ (left) and chemical structures of Eu(III) complex with oxygen-insensitive emission and Pt(II) porphyrin with oxygen-sensitive emission (right). (c) Schematic energy diagram showing the excited state equilibrium between $^5D_0$ and T_1 (left), and chemical structure of Eu(III) complex with oxygen-sensitive emission (right). (d) Chemical structure of Eu(III) complex and chemical reaction induced by $^3O_2$ and light irradiation. (e) Chemical structure of Eu(III) complex and chemical reaction induced by $^3O_2$ and mechanical stress.

Eu(III) is also an important factor for distinguishing it from the strong auto-fluorescence of living cells.

In contrast to the light-excited oxygen reaction, we demonstrated a tribo-excited oxygen reaction using Eu(III) complexes. Eu(III) complexes show triboluminescence, which is a fascinating emission phenomenon that involves the transformation of mechanical energy to UV-visible light.[134–139] We focused on the role of Eu(III) excitation energy in excited state chemical reactions to achieve tribo-excitation.[140] Based on this concept, we prepared a Eu(III) coordination polymer with hfa and phosphine oxide ligands containing a reactive anthracene unit (bpa: 2,6-bis(diphenylphosphine oxide)anthracene). The stacked structure between single polymer chains was formed in the coordination polymer *via* hydrogen bonding. The anthracene unit in the phosphine oxide ligand was transformed to anthracene peroxide by mechanical stress, which was based on the singlet oxygen reaction initiated by energy transfer from the anthracene ligand to triplet oxygen. The oxidized anthracene ligands formed an emissive Eu(III) complex that allowed the monitoring of tribo-excited chemical reactions using luminescence spectroscopy. The tribo-chemical reaction in the "excited state" are fundamentally different from the general mechanochemical reactions in the "ground states".[141–143] Such tribo-excited chemical reactions using lanthanide coordination polymers are expected to provide a new avenue for development in the fields of physical chemistry, material chemistry, and organic chemical reactions.

4 Conclusion

In this review, we have summarized the research progress on π-conjugated Eu(III) luminophores that exhibit high brightness, and we have also discussed their physical sensing applications. The electronic and steric control of large π-conjugated ligands provides high brightness and good thermostability to Eu(III) complexes. The key design points for prominent Eu(III) complexes are ligand–ligand interactions in rigid structures and poly-aromatic-type energy donors with a long-lived T_1 state. The control of the excited state dynamics through the use of π-conjugated ligands also endows effective temperature and oxygen sensing properties. Studies on a design for luminescent Eu(III) complexes open up the frontier field of research in coordination chemistry, photochemistry, and materials science.

Conflicts of interest

There are no conflicts to declare.

Acknowledgements

This work was partially supported by grant-in-aid for grant numbers JP20H02748, JP20H04653, JP20H05197, JP20K21201, JP21K18969, and JP21J20980. This work was also supported by the Institute for Chemical Reaction Design and Discovery (ICReDD), established by the World Premier International Research Initiative (WPI) of MEXT, Japan.

References

1 M. Hu, H.-T. Feng, Y.-X. Yuan, Y.-S. Zheng and B. Z. Tang, *Coord. Chem. Rev.*, 2020, **416**, 213329.

2 Z. Xu, B. Z. Tang, Y. Wang and D. Ma, *J. Mater. Chem. C*, 2020, **8**, 2614–2642.
3 T. Chatterjee and K.-T. Wong, *Adv. Opt. Mater.*, 2019, **7**, 1800565.
4 H. Uoyama, K. Goushi, K. Shizu, H. Nomura and C. Adachi, *Nature*, 2012, **492**, 234–238.
5 T.-Y. Li, J. Wu, Z.-G. Wu, Y.-X. Zheng, J.-L. Zuo and Y. Pan, *Coord. Chem. Rev.*, 2018, **374**, 55–92.
6 J. Han, S. Guo, H. Lu, S. Liu, Q. Zhao and W. Huang, *Adv. Opt. Mater.*, 2018, **6**, 1800538.
7 M. Pan, W.-M. Liao, S.-Y. Yin, S.-S. Sun and C.-Y. Su, *Chem. Rev.*, 2018, **118**, 8889–8935.
8 M. Lu, Y. Zhang, S. Wang, J. Guo, W. W. Yu and A. L. Rogach, *Adv. Funct. Mater.*, 2019, **29**, 1902008.
9 Y. Wei, Z. Cheng and J. Lin, *Chem. Soc. Rev.*, 2019, **48**, 310–350.
10 X. Qin, X. Liu, W. Huang, M. Bettinelli and X. Liu, *Chem. Rev.*, 2017, **117**, 4488–4527.
11 G. Li, Y. Tian, Y. Zhao and J. Lin, *Chem. Soc. Rev.*, 2015, **44**, 8688–8713.
12 J. Dalal, M. Dalal, S. Devi, R. Devi, A. Hooda, A. Khatkar, V. B. Taxak and S. P. Khatkar, *J. Lumin.*, 2019, **210**, 293–302.
13 J. Dalal, M. Dalal, S. Devi, A. Hooda, A. Khatkar, V. B. Taxak and S. P. Khatkar, *J. Lumin.*, 2019, **216**, 116697.
14 J. Dalal, M. Dalal, S. Devi, P. Dhankhar, A. Hooda, A. Khatkar, V. B. Taxak and S. P. Khatkar, *Mater. Chem. Phys.*, 2020, **243**, 122631.
15 P. Phogat, S. P. Khatkar, R. K. Malik, J. Dalal, A. Hooda and V. B. Taxak, *J. Lumin.*, 2021, **234**, 117984.
16 Y. Kondo, K. Yoshiura, S. Kitera, H. Nishi, S. Oda, H. Gotoh, Y. Sasada, M. Yanai and T. Hatakeyama, *Nat. Photonics*, 2019, **13**, 678–682.
17 Y.-H. Won, O. Cho, T. Kim, D.-Y. Chung, T. Kim, H. Chung, H. Jang, J. Lee, D. Kim and E. Jang, *Nature*, 2019, **575**, 634–638.
18 H. Liao, M. Zhao, M. S. Molokeev, Q. Liu and Z. Xia, *Angew. Chem., Int. Ed.*, 2018, **57**, 11728–11731.
19 J.-C. G. Bünzli, *Coord. Chem. Rev.*, 2015, **293–294**, 19–47.
20 K. Binnemans, *Coord. Chem. Rev.*, 2015, **295**, 1–45.
21 J.-C. G. Bünzli and C. Piguet, *Chem. Soc. Rev.*, 2005, **34**, 1048–1077.
22 J.-C. G. Bünzli, *Chem. Rev.*, 2010, **110**, 2729–2755.
23 H. Xu, Q. Sun, Z. An, Y. Wei and X. Liu, *Coord. Chem. Rev.*, 2015, **293–294**, 228–249.
24 M. Gaft, R. Reisfeld and G. Panczer, *Modern Luminescence Spectroscopy of Minerals and Materials*, Springer, Heidelberg, 2nd edn, 2015.
25 W. T. Carnall, P. R. Fields and K. Rajnak, *J. Chem. Phys.*, 1968, **49**, 4450–4455.
26 K. A. Gschneidner, J.-C. G. Bünzli and V. K. Pecharsky, *Handbook on the Physics and Chemistry of Rare Earths*, Elsevier, Amsterdam, 2007, vol. 37.
27 K. Binnemans, *Handb. Phys. Chem. Rare Earths*, 2005, **35**, 107–272.
28 A. F. Kirby and F. S. Richardson, *J. Phys. Chem.*, 1983, **87**, 2544–2556.
29 M. Tsurui, Y. Kitagawa, K. Fushimi, M. Gon, K. Tanaka and Y. Hasegawa, *Dalton Trans.*, 2020, **49**, 5352–5361.
30 E. E. S. Teotonio, G. M. Fett, H. F. Brito, W. M. Faustino, G. F. de Sá, M. C. F. C. Felinto and R. H. A. Santos, *J. Lumin.*, 2008, **128**, 190–198.
31 K. Yanagisawa, T. Nakanishi, Y. Kitagawa, T. Seki, T. Akama, M. Kobayashi, T. Taketsugu, H. Ito, K. Fushimi and Y. Hasegawa, *Eur. J. Inorg. Chem.*, 2015, **2015**, 4769–4774.
32 N. B. D. Lima, S. M. C. Gonçalves, S. A. Júnior and A. M. Simas, *Sci. Rep.*, 2013, **3**, 2395–2402.
33 Y. Hasegawa, K. Murakoshi, Y. Wada, S. Yanagida, J.-H. Kim, N. Nakashima and T. Yamanaka, *Chem. Phys. Lett.*, 1996, **248**, 8–12.
34 A. Beeby, I. M. Clarkson, R. S. Dickins, S. Faulkner, D. Parker, L. Royle, A. S. de Sousa, J. A. G. Williams and M. Woods, *J. Chem. Soc., Perkin Trans. 2*, 1999, 493–504.
35 Y. Hasegawa, M. Yamamuro, Y. Wada, N. Kanehisa, Y. Kai and S. Yanagida, *J. Phys. Chem. A*, 2003, **107**, 1697–1702.
36 N. Nijegorodov, V. Ramachandran and D. P. Winkoun, *Spectrochim. Acta, Part A*, 1997, **53**, 1813.
37 S. I. Weissman, *J. Chem. Phys.*, 1942, **10**, 214–217.
38 S. Sato and M. Wada, *Bull. Chem. Soc. Jpn.*, 1970, **43**, 1955–1962.
39 M. Latva, H. Takalo, V.-M. Mukkala, C. Matachescu, J. C. Rodríguez-Ubis and J. Kankare, *J. Lumin.*, 1997, **75**, 149–169.
40 J. R. Darwent, W. Dong, C. D. Flint and N. W. Sharpe, *J. Chem. Soc., Faraday Trans.*, 1993, **89**, 873–880.
41 M. L. P. Reddy, V. Divya and R. Pavithran, *Dalton Trans.*, 2013, **42**, 15249–15262.
42 C. Lee, W. Yang and R. G. Parr, *Phys. Rev. B*, 1988, **37**, 785–789.
43 A. D. Becke, *J. Chem. Phys.*, 1993, **98**, 5648–5652.
44 Y. Kitagawa, R. Ohno, T. Nakanishi, K. Fushimi and Y. Hasegawa, *Phys. Chem. Chem. Phys.*, 2016, **18**, 31012–31016.
45 M. Kasha, *Chem. Rev.*, 1947, **41**, 401–419.
46 K. Palewska and H. Chojnacki, *Mol. Cryst. Liq. Cryst.*, 1993, **229**, 31–36.
47 D. D. Morgan, D. Warshawsky and T. Atkinson, *Photochem. Photobiol.*, 1977, **25**, 31–38.
48 H. Okamoto, M. Yamaji, S. Gohda, K. Sato, H. Sugino and K. Satake, *Res. Chem. Intermed.*, 2013, **39**, 147–159.
49 F. J. Steemers, W. Verboom, D. N. Reinhoudt, E. B. van der Tol and J. W. Verhoeven, *J. Am. Chem. Soc.*, 1995, **117**, 9408–9414.
50 O. Pietraszkiewicz, S. Mal, M. Pietraszkiewicz, M. Maciejczyk, I. Czerski, T. Borowiak, G. Dutkiewicz, O. Drobchak, L. Penninck, J. Beeckman and K. Neyts, *J. Photochem. Photobiol., A*, 2012, **250**, 85–91.
51 S. I. Klink, L. Grave, D. N. Reinhoudt, F. C. van Veggel, M. H. V. Werts, F. A. J. Geurts and J. W. Hofstraat, *J. Phys. Chem. A*, 2000, **104**, 5457–5468.
52 Y. Kitagawa, F. Suzue, T. Nakanishi, K. Fushimi and Y. Hasegawa, *Dalton Trans.*, 2018, **47**, 7327–7332.

53 Y. Hasegawa, T. Sawanobori, Y. Kitagawa, S. Shoji, K. Fushimi, Y. Nakasaka, T. Masuda and I. Hisaki, *ChemPlusChem*, 2020, **85**, 1989–1993.

54 F. J. Steemers, H. G. Meuris, W. Verboom, D. N. Reinhoudt, E. B. van Der Tol and J. W. Verhoeven, *J. Org. Chem.*, 1997, **62**, 4229–4235.

55 Y. Kitagawa, M. Kumagai, T. Nakanishi, K. Fushimi and Y. Hasegawa, *Inorg. Chem.*, 2020, **59**, 5865–5871.

56 Y. Kitagawa, M. Kumagai, P. P. Ferreira da Rosa, K. Fushimi and Y. Hasegawa, *Chem. – Eur. J.*, 2021, **27**, 264–269.

57 Y. Kitagawa, M. Kumagai, P. P. Ferreira da Rosa, K. Fushimi and Y. Hasegawa, *Dalton Trans.*, 2020, **49**, 3098–3101.

58 M. Planells, E. Klampaftis, M. Congiu, R. Shivanna, K. V. Rao, O. Chepelin, A. C. Jones, B. S. Richards, S. J. George, K. S. Narayan and N. Robertson, *Eur. J. Inorg. Chem.*, 2014, **2014**, 3095–3100.

59 Y. Kitagawa, F. Suzue, T. Nakanishi, K. Fushimi, T. Seki, H. Ito and Y. Hasegawa, *Commun. Chem.*, 2020, **3**, 3.

60 G.-J. Chen, X. Qiao, J.-L. Tian, J.-Y. Xu, W. Gu, X. Liu and S.-P. Yan, *Dalton Trans.*, 2010, **39**, 10637–10643.

61 H. Song, C. Fan, R. Wang, Z. Wang and S. Pu, *J. Coord. Chem.*, 2020, **73**, 2311–2327.

62 Z. Abbas, P. Singh, S. Dasari, S. Sivakumar and A. K. Patra, *New J. Chem.*, 2020, **44**, 15685–15697.

63 Y. Kitagawa, M. Kumagai, K. Fushimi and Y. Hasegawa, *Chem. Phys. Lett.*, 2020, **749**, 137437.

64 S. Dasari, S. Singh, S. Sivakumar and A. K. Patra, *Chem. – Eur. J.*, 2016, **22**, 17387–17396.

65 D. Qiang, X. Yang, X. Deng and H.-L. Sun, *CrystEngComm*, 2016, **18**, 8159–8163.

66 T.-A. Uchida, K. Nozaki and M. Iwamura, *Chem. –Asian J.*, 2016, **11**, 2415–2422.

67 S. Dasari and A. K. Patra, *Dalton Trans.*, 2015, **44**, 19844–19855.

68 L.-N. Zhang, A.-L. Liu, Y.-X. Liu, J.-X. Shen, C.-X. Du and H.-W. Hou, *Inorg. Chem. Commun.*, 2015, **56**, 137–140.

69 Z. Weng, D. Liu, Z. Chen, H. Zou, S. Qin and F. Liang, *Cryst. Growth Des.*, 2009, **9**, 4163–4170.

70 X. Li, D. Zhang and J. Li, *Spectrochim. Acta, Part A*, 2014, **127**, 1–9.

71 L. Wang, B. Li, L. Zhang, P. Li and H. Jiang, *Dyes Pigm.*, 2013, **97**, 26–31.

72 K. Gislason and S. T. Sigurdsson, *Bioorg. Med. Chem. Lett.*, 2013, **23**, 264–267.

73 S. Deslandes, C. Galaup, R. Poole, B. Mestre-Voegtlé, S. Soldevila, N. Leygue, H. Bazin, L. Lamarque and C. Picard, *Org. Biomol. Chem.*, 2012, **10**, 8509–8523.

74 N. Petkova, S. Gutzov, N. Lesev, S. Kaloyanova, S. Stoyanov and T. Deligeorgiev, *Opt. Mater.*, 2011, **33**, 1715–1720.

75 L. Zhang and B. Li, *J. Lumin.*, 2009, **129**, 1304–1308.

76 G.-L. Law, D. Parker, S. L. Richardson and K.-L. Wong, *Dalton Trans.*, 2009, 8481–8484.

77 R. Zong, G. Zhang, S. V. Eliseeva, J.-C. G. Bünzli and R. P. Thummel, *Inorg. Chem.*, 2010, **49**, 4657–4664.

78 L. Zhang, B. Li, L. Zhang and Z. Su, *ACS Appl. Mater. Interfaces*, 2009, **1**, 1852–1855.

79 E. J. New, D. Parker and R. D. Peacock, *Dalton Trans.*, 2009, 672–679.

80 R. A. Poole, F. Kiela, S. L. Richardson, P. A. Stenson and D. Parker, *Chem. Commun.*, 2006, 4084.

81 R. A. Poole, G. Bobba, M. J. Cann, J.-C. Frias, D. Parker and R. D. Peacock, *Org. Biomol. Chem.*, 2005, **3**, 1013–1024.

82 S. I. Klink, G. A. Hebbink, L. Grave, P. G. Oude Alink, F. C. van Veggel and M. H. V. Werts, *J. Phys. Chem. A*, 2002, **106**, 3681–3689.

83 A. Köhler and D. Beljonne, *Adv. Funct. Mater.*, 2004, **14**, 11–18.

84 Naphthalene ($\Delta E(S_1)$ = 31 170 cm^{-1}),[36] phenanthrene ($\Delta E(S_1)$ = 28 920 cm^{-1}),[47] [4]-helicene ($\Delta E(S_1)$ = 26 870 cm^{-1}),[46] triphenylene ($\Delta E(S_1)$ = 29 420 cm^{-1}),[47] chrysene ($\Delta E(S_1)$ = 27 750 cm^{-1}),[47] [5]-helicene ($\Delta E(S_1)$ = 25 250 cm^{-1}),[46] picene ($\Delta E(S_1)$ = 26 620 cm^{-1}),[48] [6]-helicene ($\Delta E(S_1)$ = 24 390 cm^{-1}),[46] coronene ($\Delta E(S_1)$ = 23 320 cm^{-1}),[47] and phenacene ($\Delta E(S_1)$ = 25 710 cm^{-1}).[48].

85 J. Yuan and K. Matsumoto, *Anal. Sci.*, 1996, **12**, 31–36.

86 H. Iwanaga, *J. Lumin.*, 2018, **200**, 233–239.

87 D. B. A. Raj, S. Biju and M. L. P. Reddy, *Inorg. Chem.*, 2008, **47**, 8091–8100.

88 T. Koizuka, M. Yamamoto, Y. Kitagawa, T. Nakanishi, K. Fushimi and Y. Hasegawa, *Bull. Chem. Soc. Jpn.*, 2017, **90**, 1287–1292.

89 S. Miyazaki, K. Miyata, H. Sakamoto, F. Suzue, Y. Kitagawa, Y. Hasegawa and K. Onda, *J. Phys. Chem. A*, 2020, **124**, 6601–6606.

90 M. L. P. Reddy, V. Divya and R. Pavithran, *Dalton Trans.*, 2013, **42**, 15249–15262.

91 T. Wu, C.-W. Sher, Y. Lin, C.-F. Lee, S. Liang, Y. Lu, S.-W. H. Chen, W. Guo, H.-C. Kuo and Z. Chen, *Appl. Sci.*, 2018, **8**, 1557.

92 Z. Liu, C. H. Lin, B. R. Hyun, C. W. Sher, Z. Lv, B. Luo, F. Jiang, T. Wu, C. H. Ho, H. C. Kuo and J. H. He, *Light: Sci. Appl.*, 2020, **9**, 83.

93 K. Ding, V. Avrutin, N. Izyumskaya, Ü. Özgür and H. Morkoç, *Appl. Sci.*, 2019, **9**, 1206.

94 P. He, H. H. Wang, H. G. Yan, W. Hu, J. X. Shi and M. L. Gong, *Dalton Trans.*, 2010, **39**, 8919–8924.

95 T. Koizuka, K. Yanagisawa, Y. Hirai, Y. Kitagawa, T. Nakanishi, K. Fushimi and Y. Hasegawa, *Inorg. Chem.*, 2018, **57**, 7097–7103.

96 F.-F. Chen, Z.-Q. Bian, Z.-W. Liu, D.-B. Nie, Z.-Q. Chen and C.-H. Huang, *Inorg. Chem.*, 2008, **47**, 2507–2513.

97 Y. Yamazaki and O. Ishitani, *Chem. Sci.*, 2018, **9**, 1031–1041.

98 T. K. K. Nonomura, N. J. Jeon, F. Giordano, A. Abate, S. Uchida, T. Kubo, S. I. Seok, M. K. Nazeeruddin, A. Hagfeldt, M. Grätzel and H. Segawa, *Nat. Commun.*, 2015, **6**, 8834.

99 Y. Sasaki, S. Amemori, H. Kouno, N. Yanai and N. Kimizuka, *J. Mater. Chem. C*, 2017, **5**, 5063–5067.

100 S. Quici, M. Cavazzini, G. Marzanni, G. Accorsi, N. Armaroli, B. Ventura and F. Barigelletti, *Inorg. Chem.*, 2005, **44**, 529–537.

101 T. J. Sørensen, A. M. Kenwright and S. Faulkner, *Chem. Sci.*, 2015, **6**, 2054–2059.

102 At the present stage, the existence or non-existence of effective energy transfer process from S_1 state to ^5D_J (J = 0, 1, and 2) is unknown, but the energy transfer process *via* triplet states is confirmed by the emission lifetime depending on oxygen concentration.[59]

103 X.-D. Wang, O. S. Wolfbeis and R. J. Meier, *Chem. Soc. Rev.*, 2013, **42**, 7834–7869.

104 Y. Cui, F. Zhu, B. Chen and G. Qian, *Chem. Commun.*, 2015, **51**, 7420–7431.

105 J. Rocha, C. D. S. Brites and L. D. Carlos, *Chem. - Eur. J.*, 2016, **22**, 14782–14795.

106 W. P. Lustig, S. Mukherjee, N. D. Rudd, A. V. Desai, J. Li and S. K. Ghosh, *Chem. Soc. Rev.*, 2017, **46**, 3242–3285.

107 L. Bellucci, G. Bottaro, L. Labella, V. Causin, F. Marchetti, S. Samaritani, D. Belli Dell'Amico and L. Armelao, *Inorg. Chem.*, 2020, **59**, 18156–18167.

108 H. Peng, M. I. J. Stich, J. Yu, L.-N. Sun, L. H. Fischer and O. S. Wolfbeis, *Adv. Mater.*, 2010, **22**, 716–719.

109 Y. Kitagawa, P. P. Ferreira da Rosa and Y. Hasegawa, *Dalton Trans.*, 2021, **50**, 14978–14984.

110 Y. Cui, H. Xu, Y. Yue, Z. Guo, J. Yu, Z. Chen, J. Gao, Y. Yang, G. Qian and B. Chen, *J. Am. Chem. Soc.*, 2012, **134**, 3979–3982.

111 K. Miyata, Y. Konno, T. Nakanishi, A. Kobayashi, M. Kato, K. Fushimi and Y. Hasegawa, *Angew. Chem., Int. Ed.*, 2013, **52**, 6413–6416.

112 M. Tropiano and S. Faulkner, *Chem. Commun.*, 2014, **50**, 4696–4698.

113 R. Boddula, K. Singh, S. Giri and S. Vaidyanathan, *Inorg. Chem.*, 2017, **56**, 10127–10130.

114 R. Devi, M. Rajendran, K. Singh, R. Pal and S. Vaidyanathan, *J. Mater. Chem. C*, 2021, **9**, 6618–6633.

115 R. Boddula, J. Tagare, K. Singh and S. Vaidyanathan, *Mater. Chem. Front.*, 2021, **5**, 3159–3175.

116 M. Rajendran, R. Devi, S. Mund, K. Singh and S. Vaidyanathan, *J. Mater. Chem. C*, 2021, **9**, 15034–15046.

117 R. Devi, K. Singh and S. Vaidyanathan, *J. Mater. Chem. C*, 2020, **8**, 8643–8653.

118 R. Devi, R. Boddula, J. Tagare, A. B. Kajjam, K. Singh and S. Vaidyanathan, *J. Mater. Chem. C*, 2020, **8**, 11715–11726.

119 R. Devi and S. Vaidyanthan, *Dalton Trans.*, 2020, **49**, 6205–6219.

120 B. Rajamouli, R. Devi, A. Mohanty, V. Krishnan and S. Vaidyanathan, *New J. Chem.*, 2017, **41**, 9826–9839.

121 B. Rajamouli and V. Sivakumar, *New J. Chem.*, 2017, **41**, 1017–1027.

122 K. Singh, R. Boddula and S. Vaidyanathan, *Inorg. Chem.*, 2017, **56**, 9376–9390.

123 B. Rajamouli, P. Sood, S. Giri, V. Krishnan and S. Vaidyanathan, *Eur. J. Inorg. Chem.*, 2016, **2016**, 3900–3911.

124 B. Rajamouli and V. Sivakumar, *J. Photochem. Photobiol., A*, 2017, **347**, 26–40.

125 X.-D. Wang and O. S. Wolfbeis, *Chem. Soc. Rev.*, 2014, **43**, 3666–3761.

126 B. M. Luby, C. D. Walsh and G. Zheng, *Angew. Chem., Int. Ed.*, 2019, **58**, 2558–2569.

127 J. W. Gregory, H. Sakaue, T. Liu and J. P. Sullivan, *Annu. Rev. Fluid. Mech.*, 2014, **46**, 303–330.

128 T. Yoshihara, Y. Hirakawa, M. Hosaka, M. Nangaku and S. Tobita, *J. Photochem. Photobiol., C*, 2017, **30**, 71–95.

129 Y. Amao, *Microchim. Acta*, 2003, **143**, 1–12.

130 A. Ruggi, F. W. B. van Leeuwen and A. H. Velders, *Coord. Chem. Rev.*, 2011, **255**, 2542–2554.

131 Y. Amao, I. Okura and T. Miyashita, *Bull. Chem. Soc. Jpn.*, 2000, **73**, 2663–2668.

132 B. Zelelow, G. E. Khalil, G. Phelan, B. Carlson, M. Gouterman, J. B. Callis and L. R. Dalton, *Sens. Actuators, B*, 2003, **96**, 304–314.

133 H. Ma, X. Wang, B. Song, L. Wang, Z. Tang, T. Luo and J. Yuan, *Dalton Trans.*, 2018, **47**, 12852–12857.

134 X.-F. Chen, X.-H. Zhu, Y.-H. Xu, S. S. S. Raj, S. Öztürk, H.-K. Fun, J. Ma and X.-Z. You, *J. Mater. Chem.*, 1999, **9**, 2919–2922.

135 S. V. Eliseeva, D. N. Pleshkov, K. A. Lyssenko, L. S. Lepnev, J.-C. G. Bünzli and N. P. Kuzmina, *Inorg. Chem.*, 2010, **49**, 9300–9311.

136 Y. Hirai, T. Nakanishi, Y. Kitagawa, K. Fushimi, T. Seki, H. Ito and Y. Hasegawa, *Angew. Chem., Int. Ed.*, 2017, **56**, 7171–7175.

137 C. R. Hurt, N. Mcavoy, S. Bjorklund and N. Filipescu, *Nature*, 1966, **212**, 179–180.

138 L. M. Sweeting and A. L. Rheingold, *J. Am. Chem. Soc.*, 1987, **109**, 2652–2658.

139 Y. Hasegawa, R. Hieda, K. Miyata, T. Nakagawa and T. Kawai, *Eur. J. Inorg. Chem.*, 2011, **2011**, 4978–4984.

140 Y. Kitagawa, A. Naito, K. Fushimi and Y. Hasegawa, *Chem. - Eur. J.*, 2021, **27**, 2279–2283.

141 G.-W. Wang, *Chem. Soc. Rev.*, 2013, **42**, 7668–7700.

142 D. Tan and T. Friščić, *Eur. J. Org. Chem.*, 2018, **2018**, 18–33.

143 T. Friščić, C. Mottillo and H. M. Titi, *Angew. Chem., Int. Ed.*, 2020, **59**, 1018–1029.